

1 **Katdetectr: utilising unsupervised changepoint analysis for robust kataegis detection**

2

3 Daan M. Hazelaar^{1,2,†}, Job van Riet^{1-3,†}, Youri Hoogstrate^{1,4}, Martijn P. Lolkema² and Harmen
4 J. G. van de Werken^{1,3,5}

5

6

7 ¹Cancer Computational Biology Centre, Erasmus MC Cancer Institute, Erasmus University
8 Medical Centre, Dr. Molewaterplein 40, 3015 GD, Rotterdam, the Netherlands, ²Department
9 of Medical Oncology, Erasmus MC Cancer Institute, Erasmus University Medical Centre, Dr.
10 Molewaterplein 40, 3015 GD, Rotterdam, the Netherlands, ³Department of Urology,
11 Erasmus MC Cancer Institute, Erasmus University Medical Centre, Dr. Molewaterplein 40,
12 3015 GD, Rotterdam, the Netherlands, ⁴Department of Neurology, Erasmus MC Cancer
13 Institute, Erasmus University Medical Center, Dr. Molewaterplein 40, 3015 GD, Rotterdam,
14 the Netherlands, ⁵Department of Immunology, Erasmus MC Cancer Institute, Erasmus
15 University Medical Center, Dr. Molewaterplein 40, 3015 GD, Rotterdam, the Netherlands.

16

17 [†]Shared first-author

18

19 All Authors have seen and approved this manuscript.

20 **Abstract**

21 **Motivation:**

22 Kataegis refers to the occurrence of regional hypermutation in cancer genomes and is a
23 phenomenon that has been observed in a wide range of malignancies. Robust detection of
24 kataegis is necessary to advance research regarding the origins and clinical impact of
25 kataegis. Multiple kataegis detection packages are publicly available; however, the
26 performance of their respective approaches have not been evaluated extensively. Here, we
27 introduce katdetectr, an R-based, open-source, computationally fast, and robust package
28 for the detection, characterisation and visualisation of kataegis.

29 **Results:**

30 The performance of katdetectr and five publicly available packages for kataegis detection
31 were evaluated using an in-house generated synthetic dataset and an *a priori* labelled pan-
32 cancer dataset of whole genome sequenced malignancies. The performance evaluation
33 revealed that katdetectr has the highest accuracy and normalized Matthews Correlation
34 Coefficient for kataegis classification on both the synthetic and the *a priori* labelled dataset.
35 Katdetectr is in particularly more robust for kataegis detection within samples with a high
36 tumour mutational burden.

37 **Availability and Implementation:**

38 Katdetectr imports standardised variant calling formats (MAF and VCF) as well as standard
39 Bioconductor classes (GRanges and VRanges). Katdetectr segments genomic variants
40 utilising unsupervised changepoint detection and the Pruned Exact Linear Time search
41 algorithm. The implementation of changepoint detection utilised by katdetectr results in
42 fast computation. Furthermore, katdetectr is available on Bioconductor which ensures
43 reliability, and operability on common operating systems (Windows, macOS and Linux).

44 Katdetectr is available on Bioconductor at

45 <https://www.bioconductor.org/packages/devel/bioc/html/katdetectr.html>.

46 **Contact:** h.vandewerken@erasmusmc.nl

47 **Introduction**

48 Next-generation sequencing of cancer genomes has revealed that mutations can cluster
49 together, i.e., the acquired mutations are found in proximity to one another, much closer
50 than would be expected if they had been dispersed uniformly throughout the genome
51 purely by chance (Alexandrov et al., 2013a; Nik-Zainal et al., 2012a). This phenomenon was
52 termed kataegis and its respective genomic location was termed a kataegis foci. Kataegis,
53 which is Greek for thunderstorm or shower, was first observed and visualised in whole
54 genome sequencing (WGS) data of 21 primary breast cancers (Nik-Zainal et al., 2012b).
55 Alexandrov et al. subsequently detected 873 kataegis foci in a pan-cancer dataset containing
56 507 WGS samples from primary malignancies (Alexandrov et al., 2013b).

57

58 Extensive exploration of the aetiology of kataegis revealed a significant positive correlation
59 between kataegis and two distinct mutational signatures both attributed to the APOBEC
60 enzyme-family Alexandrov et al., 2020; Bergstrom, Luebeck, et al., 2022; Burns et al., 2013;
61 Taylor et al., 2013b).

62

63 Subsequently, multiple studies confirmed the importance of the APOBEC enzymes in cancer,
64 showing that APOBEC is a major cause of mutagenesis, both seen in clusters, dispersed
65 throughout the cancer genome and in extrachromosomal DNA (Bergstrom et al., 2021;
66 Bergstrom, Luebeck, et al., 2022; Langenbucher et al., 2021; Maciejowski et al., n.d.; Taylor
67 et al., 2013a).

68

69 Previous studies have shown that kataegis occurs within known cancer genes including
70 TP53, EGFR and BRAF which are associated with overall survival (Bergstrom, Luebeck, et al.,
71 2022). Still, the clinical significance of kataegis remains to be validated and therefore
72 obfuscates kataegis as a clinical biomarker for predicting prognosis. Nevertheless, any future
73 clinical application requires accurate and robust detection of kataegis.

74

75 Here, we introduce katdetectr, an R-based and Bioconductor package that contains a
76 complete suite for the detection, characterisation and visualisation of kataegis. Additionally,
77 we have evaluated the performance of katdetectr and five publicly available kataegis
78 detection packages (Bergstrom, Kundu, et al., 2022; Lin et al., 2021; Lora, 2016; Mayakonda
79 et al., 2018; Yousif et al., 2020).

80

81 **Approach**

82 Katdetectr was programmed in the R statistical programming language (v4.1.2) (R Core
83 Team, 2022). Briefly, katdetectr can import standardised formats denoting genomic variants
84 including: Variant Calling Format (VCF), Mutation Annotation Format (MAF) and VRanges
85 objects. Per sample, the genomic variants are pre-processed and subsequently the
86 upstream-oriented intermutation distance (IMD) is calculated (Nik-Zainal et al., 2012a). The
87 distribution of IMDs is then segmented based on unsupervised detection of changepoints
88 using the changepoint package (v2.2.3) and the Pruned Exact Linear Time (PELT) search
89 method (Haynes et al., 2017; Haynes & Killick, 2021; Killick et al., 2012; Killick & Eckley,
90 2014).

91

92 After segmentation, putative kataegis foci are called based on the following definition: 1) a
93 continuous segment harbouring ≥ 6 variants and 2) the captured IMDs within the segment

94 contain a mean IMD of ≤ 1000 bp (Alexandrov et al., 2013a). Moreover, katdetectr can
95 visualise the IMD, changepoints and their continuous segments and can highlight all
96 putative kataegis foci within a sample using an intuitive rainfall plot (Figure 1).
97 The output of katdetectr consists of an S4 object containing the putative kataegis foci
98 (GRanges), the annotated genomic variants (VRanges) and the annotated segments
99 (GRanges).

100

101 See supplementary note 1 for an extended description of the design of katdetectr and
102 parameters settings.

103

104 Figure 1, Overview of the katdetectr workflow, Intermutation distance and rainfall plots. A)
105 General workflow of katdetectr represented by arrows. B) The intermutation distance (IMD)
106 is determined for each two subsequent genomic variants per chromosome and rainfall plots
107 are used to visualise these IMDs and corresponding detected changepoint segments. C)
108 Rainfall plot of PD7049a (breast cancer) from the Alexandrov dataset as interrogated by
109 katdetectr (Alexandrov et al., 2013a). Y-axis: IMD, x-axis: variant ID ordered on genomic
110 appearance, light blue rectangles: kataegis foci with genomic variants within kataegis foci
111 shown in bold. The mutational type is depicted by the colour. The determined segmentation
112 (as mean IMD per segment) is shown by black horizontal solid lines whilst vertical lines
113 represent detected changepoints. Note that the first variant of a kataegis foci has a high
114 IMD due to the usage of the upstream-oriented IMD.

115

116 **Method**

117 The performance of katdetectr (v1.0.0) was compared to alternative packages by utilising an
118 in-house generated synthetic dataset containing 1024 samples and a publicly available pan-
119 cancer dataset containing 507 WGS samples with a priori labelled kataegis foci as curated by
120 Alexandrov et al. (2013) (Alexandrov et al., 2013a; Bergstrom, Kundu, et al., 2022; Lin et al.,
121 2021; Lora, 2016; Mayakonda et al., 2018; Yousif et al., 2020).

122

123 In order to quantify and compare performances, the task of kataegis detection was reduced
124 to a binary classification problem. The task of the kataegis detection packages was to
125 correctly label each variant for kataegis, i.e., whether or not a genomic variant lies within a
126 kataegis foci.

127

128 In order to assess performance related to sample-specific Tumour Mutational Burden
129 (TMB), we binned samples based on TMB. The synthetic dataset contained eight TMB
130 classes (0.1, 0.5, 1, 5, 10, 50, 100, 500) whilst the Alexandrov dataset was binned into three
131 TMB classes (low: $TMB < 0.1$, middle: $0.1 \geq TMB < 10$, high: $TMB \geq 10$).

132 Due to large class imbalance, we used the normalised Matthews Correlation Coefficient
133 (nMCC) as the main performance metric for performance evaluation (Chicco & Jurman,
134 2020).

135

136 See supplementary note 1 for an extended description of the datasets, synthetic data
137 generation and confusion matrices.

Performance kataegis classification

| Package | Reference | Language | Synthetic dataset | | | | Dataset labelled by Alexandrov et al. | | | | | |
|-----------------------|--------------------------------|----------|-------------------|------|-------------|-------------|---------------------------------------|-------------|-------------|-------------|-------------|-------------|
| | | | Accuracy | nMCC | F1 | TPR | TNR | Accuracy | nMCC | F1 | TPR | TNR |
| 1 katdetectr | Hazelar, van Riet et al., 2022 | R | <u>0.99</u> | 0.98 | <u>0.97</u> | 0.94 | 0.99 | <u>0.99</u> | <u>0.92</u> | <u>0.83</u> | 0.91 | 0.99 |
| 2 SeqKat | Taylor et al., 2013 | R | 0.84 | 0.54 | 0.02 | 0.93 | 0.84 | 0.99 | 0.85 | 0.69 | 0.59 | 0.99 |
| 3 MafTools | Mayakonda et al., 2018 | R | 0.74 | 0.53 | 0.01 | 0.96 | 0.74 | 0.99 | 0.85 | 0.66 | 0.93 | 0.99 |
| 4 SigProfilerClusters | Bergstrom, Kundu, et al., 2022 | Python | 0.65 | 0.52 | 0.01 | 0.88 | 0.65 | 0.99 | 0.84 | 0.68 | 0.66 | <u>0.99</u> |
| 5 ClusteredMutations | Lora, 2016 | R | <u>0.70</u> | 0.53 | 0.01 | <u>0.99</u> | 0.74 | 0.99 | 0.83 | 0.61 | <u>0.99</u> | 0.99 |
| 6 kataegis | Lin et al., 2021 | R | 0.99 | 0.80 | 0.52 | 0.36 | <u>0.99</u> | 0.99 | 0.56 | 0.03 | 0.02 | 0.99 |

Table 1, performance metrics of evaluated kataegis detection packages. Accuracy, normalized Matthews Correlation Coefficient (nMCC), F1 score, True Positive Rate (TPR) and True Negative Rate (TNR) of the kataegis detection packages on 1024 synthetic samples and 507 a priori labelled WGS samples (Alexandrov et al., 2013a). Rows were sorted in descending order based on nMCC score on the Alexandrov dataset (grey transparent background). For each performance metric, the highest score is underlined.

Results

Out of all evaluated packages, katdetectr revealed the highest overall accuracy and nMCC in correctly labelling kataegis foci within both the synthetic and Alexandrov et al. dataset (Table 1). The performance of all packages was found to be associated with the sample-respective TMB (Supplementary Figure 1). Performance evaluation per TMB-binned category revealed that katdetectr is on par with alternative packages for samples with TMB ≤ 50 . However, in contrast to alternative packages, the nMCC of katdetectr remains high for samples with high TMB (ranging between 50-500; Supplementary Figures 2-3). Furthermore, katdetectr demonstrated the fastest computational runtimes of all evaluated packages (Supplementary Figures 4).

Conclusion

Here, we described katdetectr; an R-based Bioconductor package capable of the detection, characterization and visualization of putative kataegis foci within genomic variants. Performance evaluation revealed that katdetectr robustly detects kataegis in a wide range of malignancies, irrespectively of low or high TMB. Additionally, katdetectr is user-friendly and computationally inexpensive with fast runtimes. In conclusion, the robust and reproducible methodologies of katdetectr can help facilitate further research into the clinical significance and underlying biological mechanism of kataegis.

Acknowledgements

We would like to thank John Martens, Marcel Smid and Guido Jenster for their discussions, input and support. Additionally, we would like to thank Coen Berns and Yi Ping for their initial efforts on detecting kataegis.

Funding

This research received funding from the Daniel den Hoed Fonds - Cancer Computational Biology Center (DDHF-CCBC) grant.

Conflict of Interest: none declared.

Data availability

All code used for the performance evaluation is available on GitHub at: https://github.com/ErasmusMC-CCBC/evaluation_katdetectr. All data used in the

179 performance evaluation can be found on Zenodo at:
180 <https://zenodo.org/record/6623289#.YqBxHi8RrOo>

181

182 **References**

183 Alexandrov, L. B., Kim, J., Haradhvala, N. J., Huang, M. N., Tian Ng, A. W., Wu, Y., ... &
184 Stratton, M. R. (2020). The repertoire of mutational signatures in human cancer. *Nature*,
185 578(7793), 94-101. <https://doi.org/10.1038/s41586-020-1943-3>

186

187 Alexandrov, L. B., Nik-Zainal, S., Wedge, D. C., Aparicio, S. A., Behjati, S., Biankin, A. V., ... &
188 Stratton, M. R. (2013). Signatures of mutational processes in human cancer. *Nature*,
189 500(7463), 415-421. <https://doi.org/10.1038/nature12477>

190

191 Bergstrom, E. N., Kundu, M., Tbeileh, N., & Alexandrov, L. B. (2022). Examining clustered
192 somatic mutations with SigProfilerClusters. *bioRxiv*.
193 <https://doi.org/10.1109/BIOINFORMATICS-BTAC335>

194

195 Bergstrom, E. N., Luebeck, J., Petljak, M., Khandekar, A., Barnes, M., Zhang, T., ... &
196 Alexandrov, L. B. (2022). Mapping clustered mutations in cancer reveals APOBEC3
197 mutagenesis of ecDNA. *Nature*, 602(7897), 510-517.
198 <https://doi.org/10.1038/s41586-022-04398-6>

199

200 Bergstrom, E. N., Luebeck, J., Petljak, M., Bafna, V., Mischel, P. S., Harris, R. S., & Alexandrov,
201 L. B. (2021). Comprehensive analysis of clustered mutations in cancer reveals recurrent
202 APOBEC3 mutagenesis of ecDNA. *bioRxiv*. <https://doi.org/10.1101/2021.05.27.445689>

203

204 Burns, M. B., Lackey, L., Carpenter, M. A., Rathore, A., Land, A. M., Leonard, B., ... & Harris,
205 R. S. (2013). APOBEC3B is an enzymatic source of mutation in breast cancer. *Nature*,
206 494(7437), 366-370. <https://doi.org/10.1038/NATURE11881>

207

208 Chicco, D., & Jurman, G. (2020). The advantages of the Matthews correlation coefficient
209 (MCC) over F1 score and accuracy in binary classification evaluation. *BMC Genomics*, 21(1),
210 1–13. <https://doi.org/10.1186/s12864-019-6413-7>

211 Haynes, K., Fearnhead, P., & Eckley, I. A. (2017). A computationally efficient nonparametric
212 approach for changepoint detection. *Statistics and computing*, 27(5), 1293-1305.
213 <https://doi.org/10.1007/s11222-016-9687-5>

214

215 Haynes, K., & Killick, R. (2021). *changepoint.np*: Methods for Nonparametric Changepoint
216 Detection. <https://CRAN.R-project.org/package=changepoint.np>

217

218 Killick, R., & Eckley, I. (2014). *changepoint*: An R package for changepoint analysis. *Journal of*
219 *statistical software*, 58(3), 1-19.

220

221 Killick, R., Fearnhead, P., & Eckley, I. A. (2012). Optimal detection of changepoints with a
222 linear computational cost. *Journal of the American Statistical Association*, 107(500), 1590–
223 1598. <https://doi.org/10.1080/01621459.2012.737745>

224

225 Langenbucher, A., Bowen, D., Sakhtemani, R., Bournique, E., Wise, J. F., Zou, L., ... &
226 Lawrence, M. S. (2021). An extended APOBEC3A mutation signature in cancer. *Nature*
227 *communications*, 12(1), 1-11. <https://doi.org/10.1038/s41467-021-21891-0>

228

229 Lin, X., Hua, Y., Gu, S., Lv, L., Li, X., Chen, P., Dai, P., Hu, Y., Liu, A., & Li, J. (2021). kataegis: an
230 R package for identification and visualization of the genomic localized hypermutation
231 regions using high-throughput sequencing. *BMC Genomics*, 22(1), 1-6.
232 <https://doi.org/10.1186/s12864-021-07696-x>

233

234 Lora, D. (2016). ClusteredMutations: Location and Visualization of Clustered Somatic
235 Mutations. <https://CRAN.R-project.org/package=ClusteredMutations>

236 Maciejowski, J., Chatzilipli, A., Dananberg, A., Chu, K., Toufektchan, E., Klimczak, L. J., ... & de
237

238 Lange, T. (2020). APOBEC3-dependent kataegis and TREX1-driven chromothripsis during
239 telomere crisis. *Nature genetics*, 52(9), 884-890.
240 <https://doi.org/10.1038/s41588-020-0667-5>

241

242 Mayakonda, A., Lin, D. C., Assenov, Y., Plass, C., & Koeffler, H. P. (2018). Maftools: efficient
243 and comprehensive analysis of somatic variants in cancer. *Genome research*, 28(11), 1747-
244 1756. <https://doi.org/10.1101/gr.239244.118>

245

246 Nik-Zainal, S., Alexandrov, L. B., Wedge, D. C., Van Loo, P., Greenman, C. D., Raine, K., ... &
247 Breast Cancer Working Group of the International Cancer Genome Consortium. (2012).
248 Mutational processes molding the genomes of 21 breast cancers. *Cell*, 149(5), 979-993.
249 <https://doi.org/10.1016/j.cell.2012.04.024>

250

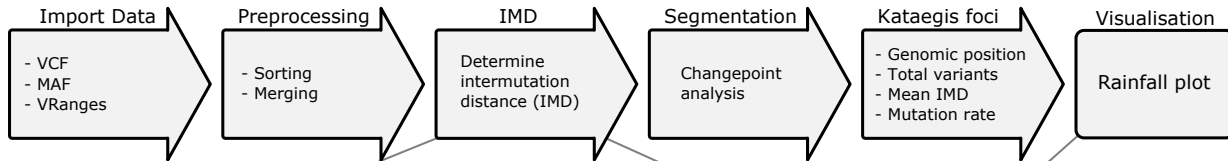
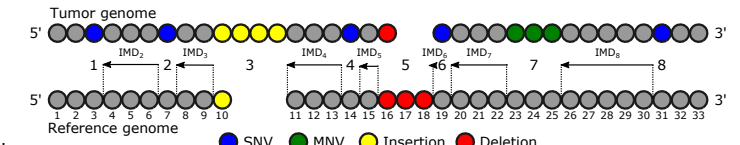
251 R Core Team. (2022). R: A Language and Environment for Statistical Computing.
252 <https://www.R-project.org/>

253

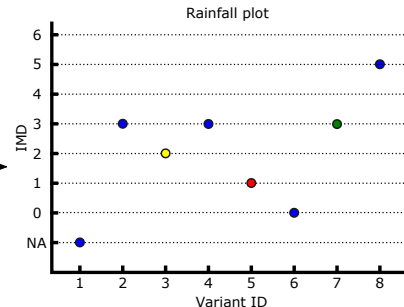
254 Taylor, B. J., Nik-Zainal, S., Wu, Y. L., Stebbings, L. A., Raine, K., Campbell, P. J., ... &
255 Neuberger, M. S. (2013). DNA deaminases induce break-associated mutation showers with
256 implication of APOBEC3B and 3A in breast cancer kataegis. *eLife*, 2.
257 doi: 10.7554/eLife.00534

258

259 Yousif, F., Lin, X., Fan, F., Lalansingh, C., & Macdonald, J. (2020). SeqKat: Detection of
260 Kataegis. <https://CRAN.R-project.org/package=SeqKat>

A**B**

| Variant ID | Type | Range | IMD |
|------------|-----------|---------|-----|
| 1 | SNV | 3-3-1 | NA |
| 2 | SNV | 7-7-1 | 3 |
| 3 | Insertion | 10-10-1 | 2 |
| 4 | SNV | 14-14-1 | 3 |
| 5 | Deletion | 16-18-3 | 1 |
| 6 | SNV | 19-19-1 | 0 |
| 7 | MNV | 23-25-3 | 3 |
| 8 | SNV | 31-31-1 | 5 |

**C**